



Cite this: *Chem. Commun.*, 2019, 55, 15129

Received 3rd October 2019,  
Accepted 5th November 2019

DOI: 10.1039/c9cc07759f

rs.c.li/chemcomm

# Reaction-based indicator displacement assay (RIA) for the development of a triggered release system capable of biofilm inhibition†

Bethany L. Patenall,<sup>‡a</sup> George T. Williams,<sup>‡a</sup> Lauren Gwynne,<sup>‡a</sup> Liam J. Stephens,<sup>‡a</sup> Emma V. Lampard,<sup>‡a</sup> Hollie J. Hathaway,<sup>‡b</sup> Naing T. Thet,<sup>a</sup> Amber E. Young,<sup>c</sup> Mark J. Sutton,<sup>d</sup> Robert D. Short,<sup>d</sup> Steven D. Bull,<sup>a</sup> Tony D. James,<sup>‡a</sup> Adam C. Sedgwick<sup>‡\*e</sup> and A. Toby A. Jenkins<sup>‡a</sup>

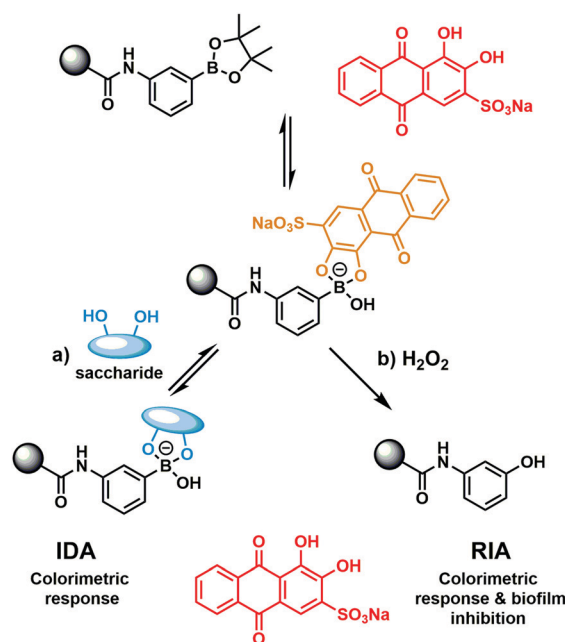
Here, a reaction-based indicator displacement hydrogel assay (RIA) was developed for the detection of hydrogen peroxide ( $H_2O_2$ ) via the oxidative release of the optical reporter Alizarin Red S (ARS). In the presence of  $H_2O_2$ , the RIA system displayed potent biofilm inhibition for Methicillin-resistant *Staphylococcus aureus* (MRSA), as shown through an *in vitro* assay quantifying antimicrobial efficacy. This work demonstrated the potential of  $H_2O_2$ -responsive hydrogels containing a covalently bound diol-based drug for controlled drug release.

Dye displacement assays exploit the chemoselective reactivity of certain chemical moieties and the reversible binding of dye molecules to a specific receptor.<sup>1</sup> Such chemistry has begun to find widespread use with marked enhancement over traditional sensing assays.<sup>1–8</sup> More complex systems containing multiple dyes also offer new paradigms for microarray development.<sup>9</sup> Not surprisingly, dye displacement assays have been elegantly employed by a number of research groups. These constructs often rely on boronic acid systems as the receptor (host) subunit with a 1,2- and 1,3-diol guest.<sup>10</sup>

Previously our group has developed boronate-based hydrogel systems as dye displacement assays (borogel) for monosaccharide detection.<sup>11,12</sup> As shown in Scheme 1, the commercially available 1,2-diol dye Alizarin Red S (ARS) was shown to successfully bind to the boronate hydrogel and result in a colour change from red to orange. Upon the addition of a monosaccharide, the

competitive displacement of ARS was observed with concomitant observation of an increase in absorption at 513 nm in solution (ARS wavelength).

Aryl boronic acids/boronate esters are well known to undergo hydrogen peroxide ( $H_2O_2$ )-mediated oxidation to form the corresponding phenol.<sup>13</sup> This unique synthetic transformation has been exploited in organic synthesis and fluorescence sensing.<sup>13</sup> We thus envisaged that modification of the previously developed ARS hydrogel bound indicator displacement assay (IDA) would yield a multimodal detection platform for the



**Scheme 1** (a) Previously developed hydrogel bound dye displacement assay (IDA) for the detection of monosaccharides.<sup>11,12</sup> (b) Present work – the development of a hydrogel bound reaction-based indicator displacement (RIA) assay for the detection of  $H_2O_2$  and for the inhibition of MRSA biofilm formation.

<sup>a</sup> Department of Chemistry, University of Bath, Bath, BA2 7AY, UK.

E-mail: t.d.james@bath.ac.uk, A.T.A.Jenkins@bath.ac.uk

<sup>b</sup> Department of Chemistry, Lancaster University, UK

<sup>c</sup> The Scar Free Foundation Centre for Children's Burns Research, The Bristol Royal Hospital for Children, Bristol, UK

<sup>d</sup> Public Health England, Porton Down, Salisbury, Wiltshire SP4 0JG, UK

<sup>e</sup> Department of Chemistry, University of Texas at Austin, 105 East 24th Street A5300, Austin, Texas 78712-1224, USA. E-mail: a.c.sedgwick@utexas.edu

† Electronic supplementary information (ESI) available. See DOI: 10.1039/c9cc07759f

‡ Equal contribution.



detection of  $\text{H}_2\text{O}_2$  with attendant antimicrobial activity (Scheme 1).<sup>14–16</sup> Here, we report the construction of a covalently incorporated ARS polyacrylamide hydrogel that undergoes oxidative activation in the presence of  $\text{H}_2\text{O}_2$  to release ARS and afford a reaction-based indicator displacement assay (RIA).<sup>15</sup> *In vitro* antibacterial assays with Methicillin-resistant *Staphylococcus aureus* (MRSA) indicated significant activity against biofilm formation for the combination of ARS and  $\text{H}_2\text{O}_2$ .<sup>17,18</sup>

In brief, phenylboronic acid (**PBA**) and benzoxaborole (**BOB**) acrylamide monomers were synthesised as previously reported.<sup>11,12</sup> Polyacrylamide hydrogels were synthesised using water (60% w/w), acrylamide (38% w/w), methylene bisacrylamide (1% w/w), and **BOB** (1% w/w) or **PBA** (1% w/w). For qualitative purposes, hydrogel slabs containing **BOB** and **PBA** were immersed in  $2.5 \times 10^{-4}$  M ARS (PBS solution). Covalent incorporation was qualitatively measured *via* the observed colour change from red to orange, as measured against a blank hydrogel (Fig. S1 and S2, ESI†). For quantitative purposes, hydrogel cylinders (0.1 g) were immersed in a  $2.5 \times 10^{-4}$  M ARS solution (1 mL) and the UV-Vis absorption at 513 nm was measured over time. As shown in Fig. S3 and S4 (ESI†), a decrease in absorbance at 513 nm was observed, which corresponded to ARS uptake into the gel. After approximately 5 h, both **PBA** and **BOB** gels were saturated with ARS, which was indicated by no further decrease in absorbance at 513 nm. Each gel was then placed into a solution of PBS (1 mL) to wash out any unbound ARS, which was shown by an increase in absorbance at 513 nm (Fig. S5 and S6, ESI†). No further increase in absorbance was observed after 3 h, which indicated the full release of any unbound ARS from each gel.

The prepared gels were then used to evaluate the response towards  $\text{H}_2\text{O}_2$ . Each gel (**PBA** and **BOB**) was placed into a solution of PBS (1 mL) and then exposed to various concentrations of  $\text{H}_2\text{O}_2$  (0–4 mM). As shown in Fig. 1 and 2, increasing

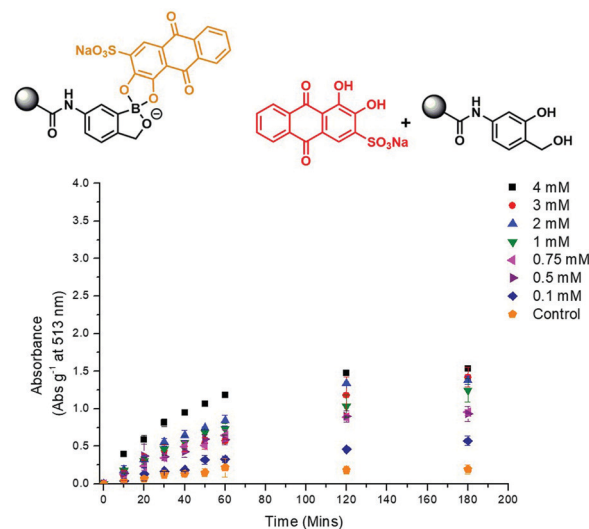


Fig. 2 UV-Vis absorption per gram of **BOB** upon addition of various concentrations of  $\text{H}_2\text{O}_2$  (0–4 mM) in PBS (pH 7.4, PBS = 0.01 M) over time (minutes). Absorbance was measured at 513 nm at 25 °C. Error bars indicate standard deviation ( $n = 3$ ).

the concentration of  $\text{H}_2\text{O}_2$  led to an increased release of ARS from the borogels, as seen in the higher absorbance at 513 nm. Interestingly, the greatest sensitivity and ARS release was observed for the **PBA**-based gels, indicative of a greater reactivity towards  $\text{H}_2\text{O}_2$  over the **BOB**-based gels (see Fig. S7 and S8, ESI†). This change in sensitivity is rationalised as the **BOB** moiety displays an enhanced binding affinity towards 1,2-diols due to an adjacent alkyl alcohol coordinating to the boron atom.<sup>12,19</sup> Therefore, we believe the adjacent methyl alcohol retards oxidation of ARS bound-boronic acid by  $\text{H}_2\text{O}_2$ .

Recent efforts by Lee and co-workers have demonstrated that alizarin ( $10 \mu\text{g mL}^{-1}$ ) is an effective inhibitor of biofilm formation for three *Staphylococcus aureus* (*S. aureus*) strains and one *Staphylococcus epidermidis* strain.<sup>20,21</sup> Biofilms are complex bacterial communities that can facilitate antibiotic resistance and impair wound healing.<sup>22</sup> Hence, the development of new systems that can effectively treat or inhibit biofilm formation are highly desirable.

$\text{H}_2\text{O}_2$  is a commonly used disinfectant and antiseptic in wound care. Therefore, we explored the potential of this system in the development of a  $\text{H}_2\text{O}_2$ -responsive hydrogel for the triggered release of ARS for biofilm inhibition against the three key stages of bacterial growth: lag, exponential and stationary. Due to the **PBA**-based gel displaying the greatest sensitivity towards  $\text{H}_2\text{O}_2$  over **BOB**-based gels (see Fig. S7 and S8, ESI†), only **PBA** gels were evaluated for biofilm inhibition. Control studies showed that the minimum inhibitory concentration (MIC) of  $\text{H}_2\text{O}_2$  was 3.5–7 mM for *Staphylococcus aureus* (*S. aureus*) H560 and MRSA252, 0.8–1.6 mM for *Pseudomonas aeruginosa* PAO1 (*P. aeruginosa* PAO1) and 3–6 mM for *Escherichia coli* NCTC 10418 (*E. coli* NCTC 10418). Unfortunately, due to poor solubility, no MIC was determined for ARS against all the bacterial strains used in this study (see Fig. S9–S11, ESI†).<sup>23–25</sup>

ARS was able to inhibit biofilm formation for *S. aureus* MRSA252 and *S. aureus* H560 at 100  $\mu\text{M}$  when added during



Fig. 1 UV-Vis absorption per gram of **PBA** upon addition of various concentrations of  $\text{H}_2\text{O}_2$  (0–4 mM) in PBS (pH 7.4, PBS = 0.01 M) over time (minutes). Absorbance was measured at 513 nm at 25 °C. Error bars indicate standard deviation ( $n = 3$ ).





**Fig. 3** Biofilm inhibition of *S. aureus* MRSA252 when treated with 2 mM H<sub>2</sub>O<sub>2</sub> and solution containing released ARS from ARS-**PBA**-based gel using 2 mM H<sub>2</sub>O<sub>2</sub> (3 h incubation). Experiments were repeated using three biological replicates, and error bars indicate standard deviation. Statistical significance of biofilm inhibition was assessed by performing a one-way ANOVA using GraphPad 7.0. \*\*\*\* $p \leq 0.001$  relative to untreated control.

the lag phase of growth (0 h), similar to other reports in the literature for Alizarin.<sup>21</sup> However, ARS was unsuccessful in the inhibition of *P. aeruginosa* PAO1 and *E. coli* NCTC 10418 biofilms at concentrations below 100  $\mu$ M (see Fig. S14–S16, ESI†). Additionally, H<sub>2</sub>O<sub>2</sub> inhibited biofilm formation, albeit at much higher concentrations, prevents growth at 5 mM for *S. aureus* MRSA252 and *S. aureus* H560, 10 mM for *E. coli* NCTC 10418, and 100 mM for *P. aeruginosa* PAO1 (see Fig. S17–S19, ESI†). H<sub>2</sub>O<sub>2</sub> (2 mM) with ARS (50  $\mu$ M) acted synergistically, effecting biofilm inhibition of *S. aureus* MRSA252 when added during the lag phase (Fig. S20, ESI†). Unfortunately, this combination was unable to inhibit biofilm formation at all other growth phases for each bacterial strain (Fig. S21 and S22, ESI†).

We next turned our attention towards the ability of the **PBA**-ARS hydrogel system to inhibit MRSA biofilm formation. Initial control experiments were carried out. **PBA**-ARS gel incubated in PBS solution for 3 h was shown to result in no biofilm inhibition, which indicates the requirement of H<sub>2</sub>O<sub>2</sub> for ARS release and no off-target gel toxicity (Fig. S23, ESI†). Control “blank” acrylamide gels were subsequently tested to evaluate the requirement of the boronic acid units for the H<sub>2</sub>O<sub>2</sub>-mediated release of ARS. Following the usual ARS-loading protocol (see ESI†), acrylamide gels loaded with ARS (ARS uptake through passive diffusion – see Fig. S2, ESI†) were treated with H<sub>2</sub>O<sub>2</sub>. No biofilm inhibition was observed, which illustrated the requirements of the boronic acid units for H<sub>2</sub>O<sub>2</sub>-mediated release of ARS from the hydrogel (Fig. S24, ESI†). To capitalize upon the H<sub>2</sub>O<sub>2</sub>-mediated release of ARS from the boronic acid containing polyacrylamide hydrogel, **PBA**-based gels (0.1 g comprising of  $2.5 \times 10^{-4}$  M ARS) were incubated with H<sub>2</sub>O<sub>2</sub> (2 mM) for 3 h to achieve maximum ARS release (*cf.* Fig. 1). The resultant ARS release was then applied to *S. aureus* MRSA252 at the lag phase. Remarkably, this resulted in complete biofilm inhibition (Fig. 3) thus demonstrating the potential of the **PBA**-based gels as a “smart” wound dressing.

In summary, we have developed a multimodal reaction-based indicator displacement (RIA) hydrogel assay for the

detection of H<sub>2</sub>O<sub>2</sub> with concomitant release of ARS for antimicrobial application. The greatest reactivity towards H<sub>2</sub>O<sub>2</sub> was observed for the **PBA**-based gel compared to the **BOB**-based gel, attributed to attenuated reactivity of the cyclic **BOB**-boronate ester. In addition, the antimicrobial efficacy of each assay component was evaluated with the aim of developing a “triggered release” antimicrobial hydrogel. ARS was discovered to be a potent biofilm inhibitor in combination with hydrogen peroxide against *S. aureus* MRSA252, with the ARS loaded **PBA**-based gel successfully inhibiting biofilm formation. These results lead us to suggest that **PBA**-based gels, in combination with an early bacterial detection system for a MRSA biomarker, might find use as a “smart” wound dressing capable of preventing MRSA biofilm formation.<sup>26</sup>

The authors would like to thank the EPSRC for grant EP/R003556/1. BLP would also like thank James Tudor and Mr and Mrs Watson for additional funding. GTW would like to thank the EPSRC and Public Health England. ACS, ATAJ and NTT wish to thank the EPSRC for funding on Smartwound plasma – EP/R003939/1. TDJ wishes to thank the Royal Society for a Wolfson Research Merit Award. We would like to thank James T. Brewster II at Harvard college for helpful discussions and suggestions to improve the manuscript.

## Conflicts of interest

No conflicts of interest.

## Notes and references

- 1 B. T. Nguyen and E. V. Anslyn, *Coord. Chem. Rev.*, 2006, **250**, 3118–3127.
- 2 A. M. Piatek, Y. J. Bomble, S. L. Wiskur and E. V. Anslyn, *J. Am. Chem. Soc.*, 2004, **126**, 6072–6077.
- 3 D. Leung, J. F. Folmer-Andersen, V. M. Lynch and E. V. Anslyn, *J. Am. Chem. Soc.*, 2008, **130**, 12318–12327.
- 4 B. T. Nguyen, S. L. Wiskur and E. V. Anslyn, *Org. Lett.*, 2004, **6**, 2499–2501.
- 5 V. Janowski and K. Severin, *Chem. Commun.*, 2011, **47**, 8521–8523.
- 6 J. H. Zhang, S. Umemoto and K. Nakatani, *J. Am. Chem. Soc.*, 2010, **132**, 3660–3661.
- 7 T. Minami, Y. L. Liu, A. Akdeniz, P. Koutnik, N. A. Esipenko, R. Nishiyabu, Y. Kubo and P. Anzenbacher, *J. Am. Chem. Soc.*, 2014, **136**, 11396–11401.
- 8 S. Comby, S. A. Tuck, L. K. Truman, O. Kotova and T. Gunnlaugsson, *Inorg. Chem.*, 2012, **51**, 10158–10168.
- 9 Y. Sasaki, Z. J. Zhang and T. Minami, *Front. Chem.*, 2019, **7**, 150, DOI: 10.3389/fchem.2019.00049.
- 10 X. Wu, Z. Li, X. X. Chen, J. S. Fossey, T. D. James and Y. B. Jiang, *Chem. Soc. Rev.*, 2013, **42**, 8032–8048.
- 11 W. M. J. Ma, M. P. P. Morais, F. D’Hooge, J. M. H. van den Elsen, J. P. L. Cox, T. D. James and J. S. Fossey, *Chem. Commun.*, 2009, 532–534.
- 12 E. V. Lampard, A. C. Sedgwick, T. Sombuttan, G. T. Williams, B. Wannalser, A. T. A. Jenkins, S. D. Bull and T. D. James, *ChemistryOpen*, 2018, **7**, 266–268.
- 13 J. Chan, S. C. Dodani and C. J. Chang, *Nat. Chem.*, 2012, **4**, 973–984.
- 14 A. Romieu, *Org. Biomol. Chem.*, 2015, **13**, 1294–1306.
- 15 X. L. Sun, M. L. Odyneec, A. C. Sedgwick, K. Lacina, S. Y. Xu, T. T. Qiang, S. D. Bull, F. Marken and T. D. James, *Org. Chem. Front.*, 2017, **4**, 1058–1062.
- 16 X. L. Sun, K. Lacina, E. C. Ramsamy, S. E. Flower, J. S. Fossey, X. H. Qian, E. V. Anslyn, S. D. Bull and T. D. James, *Chem. Sci.*, 2015, **6**, 2963–2967.
- 17 C. H. Ren, L. P. Chu, F. Huang, L. J. Yang, H. R. Fan, J. F. Liu and C. H. Yang, *RSC Adv.*, 2017, **7**, 1313–1317.



- 18 F. Liu, L. B. Bai, H. L. Zhang, H. Z. Song, L. D. Hu, Y. G. Wu and X. W. Ba, *ACS Appl. Mater. Interfaces*, 2017, **9**, 31626–31633.
- 19 M. Dowlut and D. G. Hall, *J. Am. Chem. Soc.*, 2006, **128**, 4226–4227.
- 20 J. H. Lee, Y. G. Kim, S. Y. Ryu and J. Lee, *Sci. Rep.*, 2016, **6**, 19267, DOI: 10.1038/srep19267.
- 21 R. K. Manoharan, J. H. Lee, Y. G. Kim and J. Lee, *Front. Cell. Infect. Microbiol.*, 2017, **7**, 447, DOI: 10.3389/fcimb.2017.00447.
- 22 C. W. Hall and T. F. Mah, *FEMS Microbiol. Rev.*, 2017, **41**, 276–301.
- 23 G. Zhu, Q. Wang, S. Lu and Y. Niu, *Med. Princ. Pract.*, 2017, **26**, 301–308.
- 24 G. McDonnell and A. D. Russell, *Clin. Microbiol. Rev.*, 2001, **14**, 227–228.
- 25 Y. Yamada, T. Mokudai, K. Nakamura, E. Hayashi, Y. Kawana, T. Kanno, K. Sasaki and Y. Niwano, *J. Toxicol. Sci.*, 2012, **37**, 1091.
- 26 N. T. Thet, D. R. Alves, J. E. Bean, S. Booth, J. Nzakizwanayo, A. E. R. Young, B. V. Jones and A. T. A. Jenkins, *ACS Appl. Mater. Interfaces*, 2016, **8**, 14909–14919.

